

**BLADE VIBRATION MEASUREMENTS AND EXCITATION FORCE EVALUATION**

**Nicolò Bachschmid**  
R&D Department  
Franco Tosi Meccanica  
Legnano (MI) Italy



**Emanuel Pesatori**  
Head of Engineering  
Franco Tosi Meccanica  
Legnano (MI) Italy



*Full professor of Applied Mechanic since 1986 at Politecnico di Milano, retired in 2008, actually consultant in research activities.*

**Simone Bistolfi**  
R&D Department  
Franco Tosi Meccanica  
Legnano (MI) Italy



*Head of Product Development Department since 1990*

*R&D Engineer at Franco Tosi Meccanica since 2009.*

**ABSTRACT**

Tip timing blade vibration measuring systems have become nowadays common for monitoring blade vibrations, due to rather easy and non-intrusive installation of sensors. The data collected by the sensors must be heavily processed in order to get the vibration time histories of all blades at rated speed or during a run up or run down transient. In the paper a real case of tip timing measurement for a steam turbine is shown. Resonant/natural frequencies, amplitude and phase of each blade vibration with respect to the synchronous reference, are identified. The first measurement results shown are related to asynchronous vibrations of a steam turbine last stage blade row due to an instability. The second results are instead transient synchronous vibrations when passing a blade row resonance during a run up of the steam turbine. It is further shown how synchronous vibrations, although non stationary, allowed to identify damping and excitation amplitudes by means of an original approach based on modal analysis.

**INTRODUCTION**

In the last stage of a low pressure steam turbine, during the commissioning of the plant, some cracks located just above the roots have been found in some blades after hundreds of hours of operation. In this short period the turbine ran in off-design conditions, namely at low mass flow, due to low output power, and rather high condenser pressure. Figure 1 shows two of these cracks, which were found during an inspection and after disassembling the blades. The blades, without shrouds on top, were packed in groups of 8 blades by welded lashing wires, as shown in Fig. 2. The generation of cracks has been attributed to

high vibration levels which developed at rated speed due to instability in the fluid flow coupled to a vibration mode of the pack. Such kind of instability, often called flutter instability, may occur in particular off-design operating conditions, generally in low output power and high condenser pressure conditions, as also reported in literature (see e.g. [1-5]). In [1] a last stage blade row failure due to this instability is reported and carefully analyzed, in [2] attention is paid to the occurrence of these vibrations, in [3] flutter in shrouded rotor blades has been investigated and in [4] flutter in turbine blades with cyclic symmetric modes has been studied. Finally in [5] the instability has been reproduced in a full scale test rig with air and successfully simulated by means of CFD calculations.

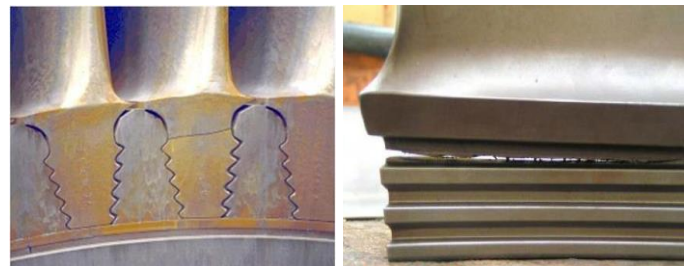


**Figure 1:** Cracks detected in the blade roots

In the case analyzed in the paper the instability was coupled to one of the natural frequencies of the single blade pack, where the corresponding mode shape could couple effectively with the pressure distribution in the unstable steam flow. It was suspected that mainly the top of the blades were involved in a reverse flow. Due to low material damping, low friction damping in the roots and the absence of friction in welded lashing wires, the blade pack experienced rather high vibration amplitudes.



**Figure 2:** Pack of 8 blades with welded lashing wires

The analysis of the instability, the measurements and the means used to overcome the problem have been fully described in [6].

### TIP TIMING TECHNOLOGY

After removal and substitution of cracked blades, a tip timing measurement system was installed on the steam turbine in order to measure blade vibrations and define safe and unsafe turbine operating conditions. A total of 7 sensors were positioned on the casing in correspondence of the blade row for detecting the blade tip passing in front of the sensor. The position of 3 sensors on the exhaust casing of the steam turbine is shown in Fig. 3: the axial position of all sensors was in correspondence of the last stage blade row.



**Figure 3:** Position of 3 sensors on the turbine exhaust casing

The tip vibration amplitude must be evaluated taking into consideration that the assumed direction of vibration is different with respect to the circumferential direction where the actual arrival time of the blade is measured. Figure 4 shows also how actual vibration amplitude can be deduced from measured apparent deflection in circumferential direction. Theoretical blade arrival time is calculated considering the position of the un-deflected blade and the shaft revolution

period. Comparing the actual arrival time with the theoretical time allows to evaluate the relative advance or delay in time and consequently, by dividing that time by the circumferential speed of the tip of the blade, its actual deflection. From different deflections measured in each revolution the blade deflection time history can be reconstructed and the vibration amplitude can be evaluated. The direction of vibration cannot be measured and must be estimated from previously performed modal analysis of the blade pack. Also the blade row or blade pack natural frequencies must be roughly known, in order to estimate the number of vibration cycles during one revolution of the shaft.

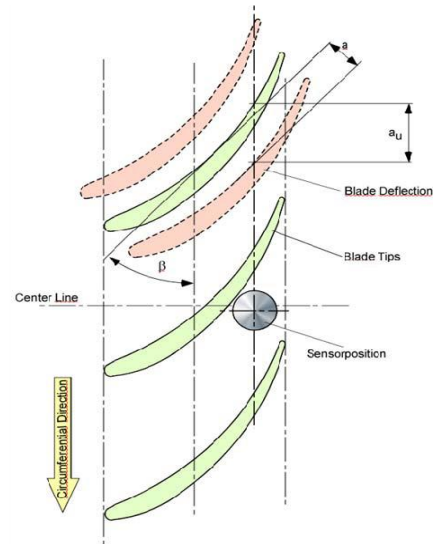


**Figure 4:** Path of blade tips and direction of vibration

Synchronous engine order vibrations show the blade always in the same deflected position. Therefore more sensors are required for getting more points of the sinusoidal vibration, and extract the maximum amplitude. Asynchronous vibrations could be measured with one sensor only, because after each revolution the position of the blade will be different, which allows to reconstruct the sinusoidal vibration and the associated frequency.

### PRELIMINARY BLADE ROW DYNAMIC ANALYSIS

The last stage of the low pressure steam turbine was composed of 120 blades, grouped in packs of 8 blades by welded lashing wires and fixed on the rotor by means of fir tree side entry roots. Taking into account also the centrifugal field, the modal analysis allowed to identify the following natural frequencies and associated modes: the 1st (tangential) mode at 115 Hz, the 2nd (axial) mode at 185 Hz and the 3rd (so called X-mode) at 225 Hz.

This last mode, shown in Fig. 5, is the vibration mode that is most likely and strongly excited as the cracks and lashing wire failures mostly developed in first and last blades of the packs. Other eigen-frequencies and associated mode shapes were not excited and are omitted.

This analysis allowed to predict the direction of vibration and the range of the associated natural frequency.

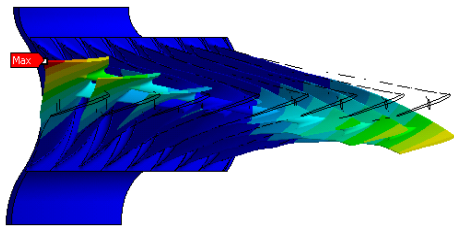


**Figure 5:** Top view of pack of 8 blades vibrating in its 3rd mode (X-mode) at 225 Hz casing

### BLADE INSTABILITY MEASUREMENT RESULTS

To avoid further blade cracks it was decided to monitor the blade vibrations for defining safe operating conditions. The instability occurred during the run up and at full speed in critical discharge pressure conditions. Figure 6 shows the deflections of blade no. 53 during the speed transient from about 2700 rpm to 2890 rpm. The blade is deflected due to centrifugal force and is vibrating at a frequency of 217 Hz, which is close to one of the natural blade pack frequencies (which was assumed to be at 225 Hz at rated speed from calculation). The corresponding pack mode is called X-mode. Resonant conditions could occur at 2700 rpm with the 5th EO excitation (as shown in Fig. 6). High vibrations are measured instead at a rotating speed of 2770 rpm, which indicates an excitation at a non-integer engine order of 4.7, which is due to the fluid-dynamic instability. Maximum peak-to-peak apparent amplitude at blade tip was 14.1 mm, which projected in the direction of vibration gives a true vibration amplitude of 4.72 mm. Maximum apparent deflection due to centrifugal force and steam was 12.5 mm

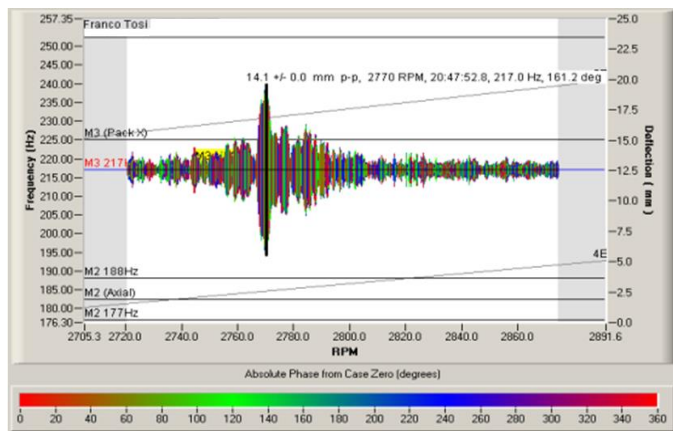


**Figure 6** Deflection and vibration of blade no. 53 at the 3rd pack natural frequency (217 Hz) during a speed transient.

Frequency remains constant as rotating speed increases, indicating non synchronous excitation or instability. Colors which indicate phase of vibration with respect to the 1x rev. reference are randomly distributed around resonance, indicating an asynchronous vibration, where the phase is random. Figure 7 shows the distribution of blade vibration amplitudes over the blade row composed of 120 blades.

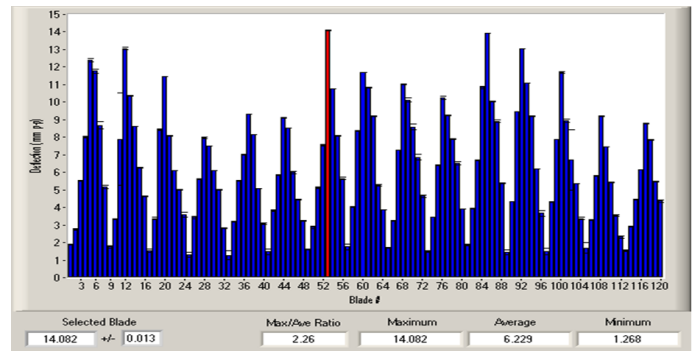


**Figure 7** Distribution of the apparent blade tip amplitude along the blade row composed by 15 packs of 8 blades each.

The vibration amplitude distribution shows clearly that maximum amplitude occurs each 8 blades: the first and the last blade of the group of 8 blades are vibrating with maximum amplitude (typical for the X-mode). These blades were also those where cracks close to the roots and lashing wire failures had been found. In the row of 120 blades there are 15 packs of 8 blades each, therefore 15 peaks and 15 nodes are found in the vibration distribution around the row, as shown in Fig. 7.

During run-down speed transients the 5th engine order excited some vibrations at 228 Hz (X-mode) for a rotational speed of 2736 rpm, the 4th engine order excited the 2nd (axial) mode at 174.3 Hz for 2610 rpm and the 1st (tangential) mode at 115 Hz was excited by engine order 3 for a rotational speed of 2300 rpm. During these resonance crossing conditions the phase variation, indicated by the gradually changing colors instead of randomly distributed colors, as in Figure 3 related to instability, was consistent with a synchronous engine order vibration.

At rated speed (3000 rpm) and rather high condenser pressure (130 mbar) with low output power (10 MW), high vibrations (shown in Figures 8 and 9) are experienced, with the same vibration mode (X-mode) and frequency (217 Hz), as in the speed transient of Figure 6. But also another vibration mode (the first axial mode of the blade pack) at 180 Hz (not related to the rotational speed) did appear.

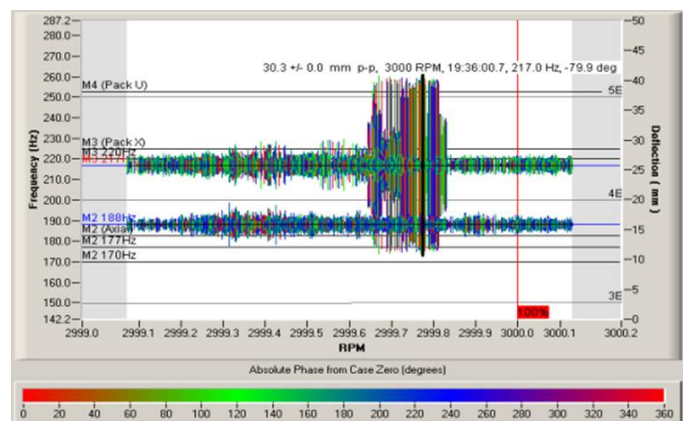


**Figure 8** Vibration of blade no. 71 which experiences maximum amplitude at rated speed.

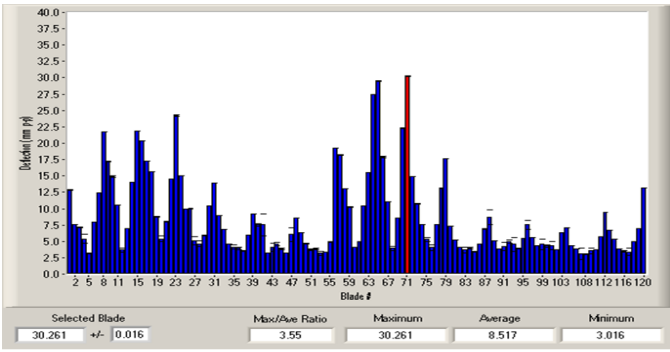


**Figure 9** Vibration amplitude distribution along the row at rated speed

Now the engine order is 4.34 and phases are changing randomly, which confirms fluid-dynamic instability. Maximum apparent vibration peak-to-peak amplitude reached 30.3 mm at tip of blade no. 71, which corresponds to a vibration amplitude of roughly 10 mm. These vibration levels are dangerous and operation in these conditions should be avoided. The turbine was operated in these conditions only for few minutes. The natural frequency value (217 Hz) at which flutter occurs is lower than the synchronous resonance value (228 Hz) measured during the run-down: this could be due to the fluid-structure interaction typical for flutter vibrations. Several tests with different values of output power and condenser pressure allowed finally to define the safe and the not-allowed operating condition fields which are shown in Figure 10.

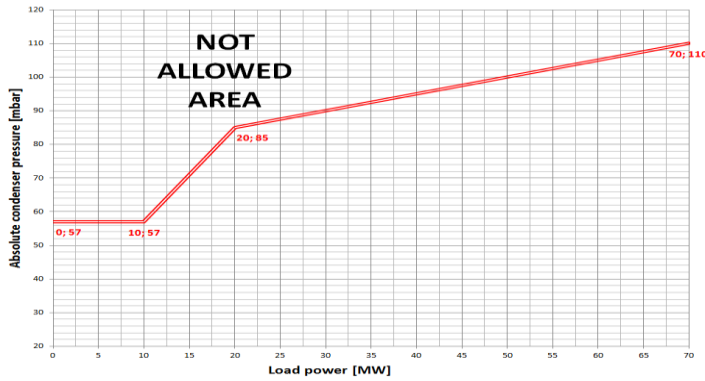


**Figure 10** Definition of safe and not-allowed operation fields.

Later a different blade row (with welded shrouds on top) was substituted to the previous one, and measurements were taken with the same tip timing system. Blades were grouped in packs of 10 blades with welded shrouds, therefore the sensors were able only to recognize the passage of the first blade of each pack instead of each blade as previously.

**MODIFIED BLADE PACK DYNAMIC BEHAVIOUR**

The design of the last stage blade has been reviewed in order to reduce its sensibility to the dangerous operating conditions where severe vibrations are excited due to instability. Blades have been shortened and blade tip has been provided

with a shroud. The casing has been modified accordingly to accommodate the blades with reduced height. This allows the backward flow at high backpressure and low load to be reduced at the tip of the blades. Blade packs have been welded in packs of 10 blades instead of 8. This increases slightly the natural frequency of the X-mode, and should reduce the coupling of the blade pack with the unstable fluid flow in this vibration mode.

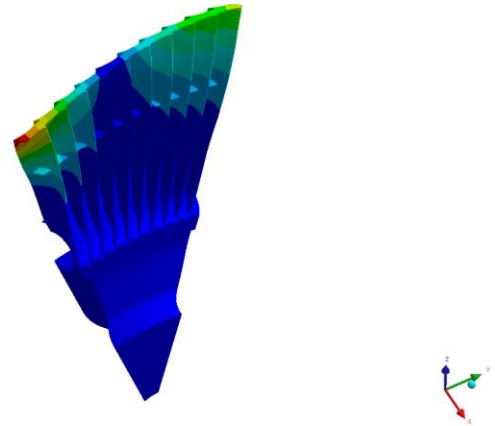


**Figure 11** Group of 10 blades with welded shrouds and snubbers, vibrating according X-mode at 240 Hz.

Figure 11 shows a group of 10 blades, vibrating in its 3rd mode (X-mode). Using cyclic symmetry the modal analysis allows the blade row natural frequencies as function of the nodal diameters to be calculated. Figure 12 shows the calculated eigenfrequencies as function of the number of the nodal diameters (or engine orders), related to the 12 groups of 10 blades: all possible engine order resonances are avoided at rated speed (light blue line) and in over-speed conditions (orange line). Integer engine order excitations do not match eigenfrequencies with corresponding number of nodal diameters.

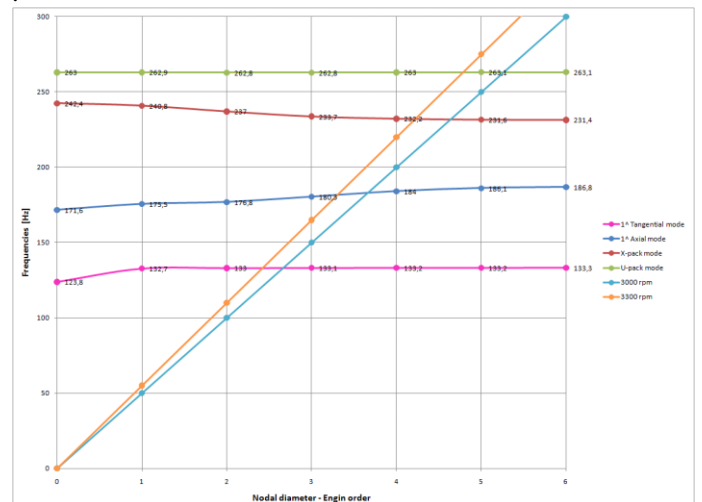


**Figure 12.** Eigenfrequencies of the first 4 blade pack modes as function of nodal diameter numbers/engine order excitation.

The Campbell diagrams allow the possible resonances to be detected during speed transients when the frequency of a

certain engine order excitation coincides with the natural frequency of a mode with the same order of nodal diameters. In Figure 13 (top) at the rotational speed of 2440 rpm, resonance occurs between engine order 3 excitation and 1st (tangential) mode with 3 nodal diameters at 122 Hz. In Figure 13 (bottom) resonance occurs at 2240 rpm between engine order 6 excitation and the 3rd X-mode with 6 nodal diameters at a frequency of 224 Hz. This last one was the vibration mode which was excited by the instability in the first version of the blade row (packets of 8 blades). Not shown is the further resonance of engine order 4 excitation with the second (axial) mode at 175 Hz and for a rotational speed of 2640 rpm.

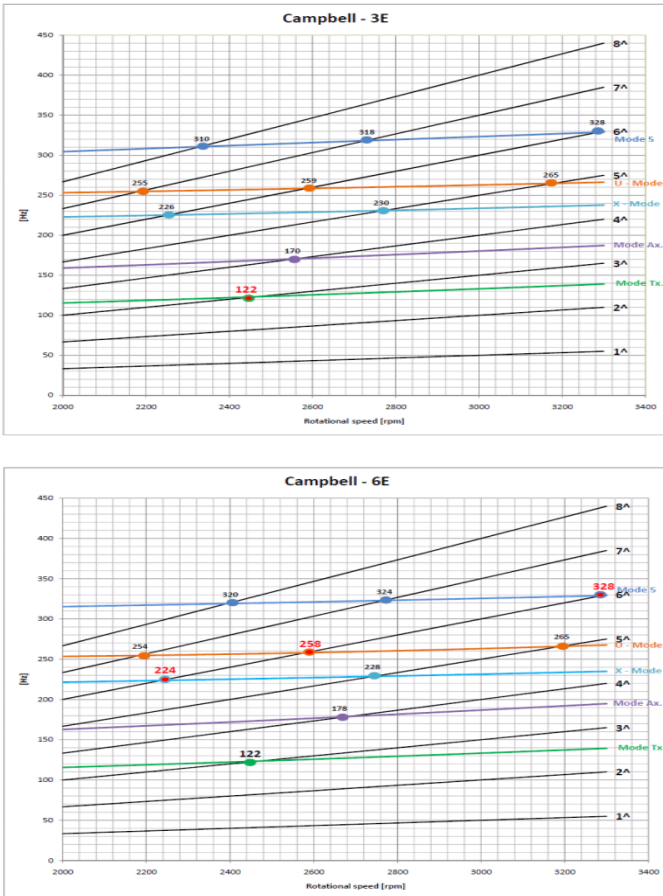


Figure 13. Campbell diagrams for modes with 3 nodal diameters (top) and 6 nodal diameters (bottom).

### BLADE ROW SYNCHRONOUS VIBRATION DURING RUN UP TRANSIENT

Figure 14 shows the vibration time histories of each pack measured at the shroud of the first blade of the pack as function of the rotational speed during the speed rise between 2207 and 2440 rpm which occurred in 7 seconds (with an acceleration of 3.48 rad/sec<sup>2</sup>).

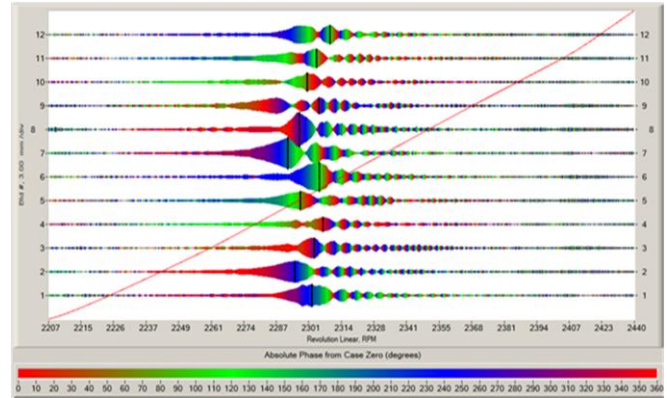


Figure 14. Passing of resonances of the 12 packs during run up transient recorded by tip timing measurements

For the shaft lateral vibration measurement the acceleration is sufficiently low to consider the transient as a sequence of steady state conditions at different rotational speeds. Colors indicate phase of vibration with respect to the 1x rev. reference, and show typical phase rotation by passing resonance. Natural frequencies, damping and even excitation seem to be slightly different from pack to pack, due to manufacturing and assembling tolerances, and to some irregularity in the excitation. Taking as reference blade pack 8 the maximum vibration amplitude is around 2 mm. Similar amplitudes are found in packs 6 and 8. In this mode the direction of the vibration is tangential that is exactly the direction of the tip timing measurement.

Being the excitation a 3rd engine order (with a 3x rev. exciting frequency) its acceleration is 10.45 rad/s<sup>2</sup> (three times the rotational acceleration). The effect of this rather high acceleration is clearly visible in the graph: the maximum peak is followed by a series of smaller peaks due to a beating phenomenon between natural and exciting frequency. Tip timing system software allows to isolate a single blade pack for a deeper analysis, as shown in Fig. 15 and Fig. 16.

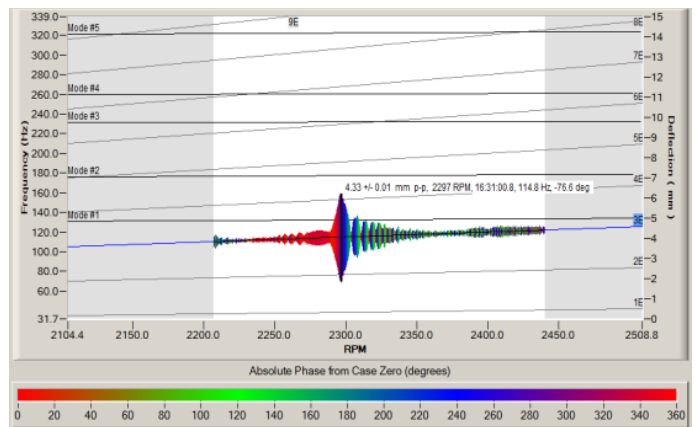
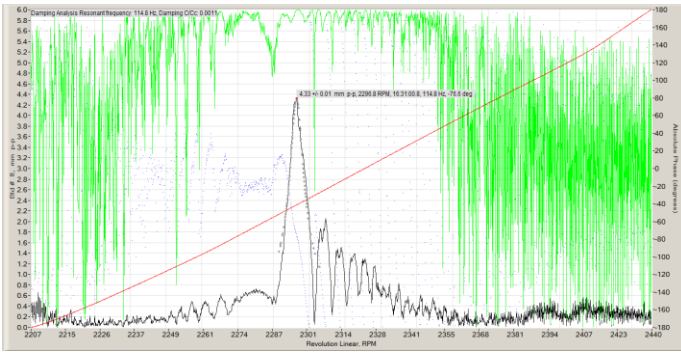


Figure 15: Blade pack nr. 8 transient vibration



**Figure 16:** Blade pack nr. 8 envelope analysis

From these experimental records both the excitation strength and the modal damping of the blade pack, which are both unknown, will be identified.

### DAMPING AND EXCITATION IDENTIFICATION

The software of the tip timing system aims also to evaluate the modal damping ratio of the blade row, by comparing measured results gathered when passing a blade row resonance with simulated results of a reduced modal model of the blade row (1 d.o.f. system). The resonant vibration must be uncoupled, then an estimate of the half power width, corrected by a least square curve fitting procedure can be used for evaluating the damping ratio.

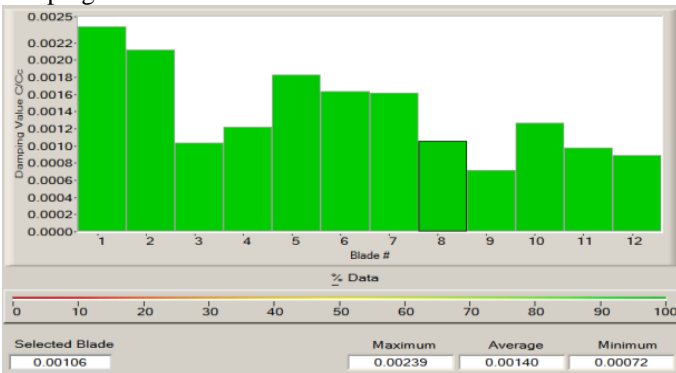


**Figure 17:** Evaluation of dimensionless damping ratio

The damping found this way resulted in between a minimum of 0.072% and a maximum of 0.239% as shown in Fig. 13. Packs 6 and 7 were around 0.16%, pack 8 was 0.106%. But the evaluation of the modal damping ratio may be rather inaccurate when the acceleration of the frequency of excitation (which is the engine order multiplied by the angular acceleration of the rotor) is not sufficiently low: in this case the resonant condition is passed during a transient and the half power width applied to the transient frequency curve is not directly applicable.

A one d.o.f. modal model of the pack has been build: from previous analysis the 1st mode natural frequencies are known, but in order to define the modal models it is useful to refer the modal mass and stiffness to a characteristic point of the 3D model. The point which has been chosen is the tip of the blades, because there vibration amplitude is maximum and has been

easily measured by tip timing methods. Each pack will therefore be represented by a lumped mass (the modal mass) located at the top of the pack in its middle position, which is connected to the shaft axis by a spring which represents the modal stiffness. In order to define the modal stiffness an approximated simple approach has been used. The blade pack is composed by blades which are deflected according to its first mode of deflection. This mode is similar to a static deflection generated by a unitary force applied to the tip of the blade clamped at its root, in tangential direction, as shown in Fig. 18. This unitary force, divided by the calculated static deflection, defines the static stiffness at the top of the blade pack, which is assumed to be the modal stiffness  $k_1$  in the first vibration mode in tangential directions. Corresponding modal mass  $m_1$  is obtained from natural frequency.

$$m_1 = k_1 \omega_1^{-2} \quad (1)$$

Fig. 19 shows how the 12 modal models are connected to the shaft, for representing the zero nodal diameter mode in tangential direction of the blade row composed by the 12 packs. The modal damping has been defined by comparing the time histories calculated with different values of damping ratios, and unit excitation, to the experimental curves: best fitting defines the modal damping.



**Figure 18:** Blade pack stiffness evaluation

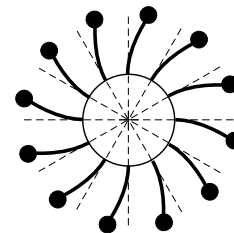


**Figure 19:** modal model of the blade row.

These time histories are obtained with the usual Runge-Kutta time integration, applied to the 1 dof system with stiffness  $k_1$  and mass  $m_1$  (natural frequency  $f_1$  equal to 122Hz), different damping ratios, unitary exciting force and acceleration through resonance equal to  $10,45 \text{ rad/s}^2$ . Being the system linear the time history shapes are independent from intensity of excitation. These curves are shown in Fig. 20 and Fig. 21: in Fig. 20 one time history with a given damping ratio and in Fig. 21 the envelope analysis giving vibration amplitude as function

of time for different modal damping ratios.

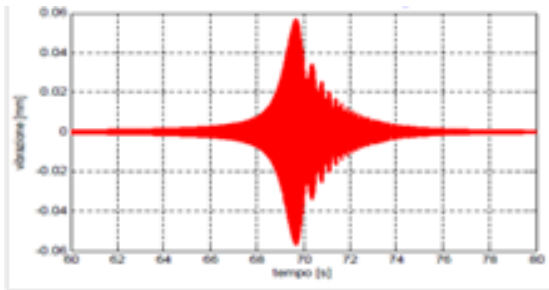


**Figure 20:** Vibration time history: accelerating through resonance

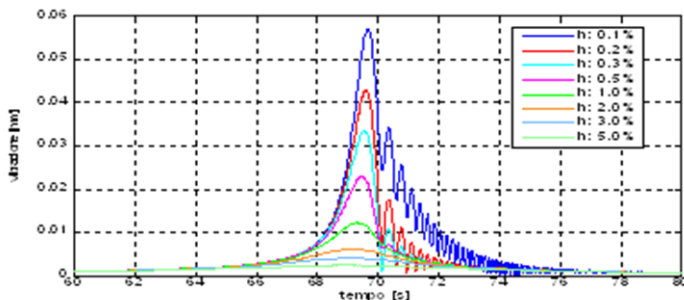


**Figure 21:** Envelope analysis of time histories with different damping values

Resulting best fitting has been found for modal damping 0.2% for pack 8 and around 0.3% for packs 6 and 7. This means that the damping evaluated by means of the half power width is heavily underestimated: real damping ratio reaches twice the value found by half power width.

Maximum amplitude of the 1 d.o.f. system with unit excitation (1 N) and 0.2% damping ratio in steady state resonant conditions would have been 63  $\mu\text{m}$ , to be compared to 42  $\mu\text{m}$  reached in the diagram of Fig. 21 during transient excitation with an acceleration is 10.45  $\text{rad/s}^2$ . With this damping ratio and the measured vibration amplitude of 2 mm (see Fig. 10) then also the excitation amplitude has been evaluated assuming proportionality: its value resulted something less than 50 N. This is the amplitude of the equivalent force applied to the top of the blade pack which produces the measured vibrations due to the 3rd component of the circumferential steam pressure distribution that cause the 3EO excitation, whose cause remains unknown.

## CONCLUSIONS

Some last blade failures in a steam turbine suggested to monitor blade vibration by means of a tip timing system. Measurement technique is described and the obtained results, which require full 3D modelling of the complete blade row, have allowed to define the operating conditions in which the turbine could be operated safely. The same tip timing measuring system has then been used for monitoring blade vibrations of the modified shrouded blade packs. During the run up transient a predicted possible blade row resonance has been excited. From time history of passing the resonance with a

consistent acceleration, modal damping and excitation severity have been identified.

It has been shown that, combining a simple measuring technique with accurate processing of the collected data and with effective 3D modelling, complex vibrational behavior can be successfully analyzed. From the collected data with the aid of simple modal models also the modal damping in operating conditions and the actual exciting forces, which are quantities that are only roughly estimated by turbine manufacturers, have been identified.

## REFERENCES

- [1] Mazur, Z., Hernandez-Rosette, A., Garcia-Illescas, R., 2006. Investigation of the failure of the L-0 blades. *Engineering Failure Analysis*, 13(8), pp. 1338-1350.
- [2] Mcbean, I., Masserey, P-A., Havakechian, S., 2010. The development of long last stage steam turbine blades. *ASME Turbo Expo 2010: Power for Land, Sea, and Air (GT2010)*, June 14–18, 2010, Glasgow, UK, paper GT2010-22747, pp. 2245-2256. doi:10.1115/GT2010-22747.
- [3] Hsiao-Wei, D.C., Chi-Chih, C., Chih-Neng, H., Gwo-Chung, T., Kwang-Lu, K., 2003. An investigation of turbomachinery shrouded rotor blade flutter. *ASME Turbo Expo 2003, International Joint Power Generation Conference (GT2003)*, June 16–19, 2003, Atlanta, Georgia, USA, pp. 331-338. doi:10.1115/GT2003-38311.
- [4] Kielb, R., Barter, J., Chernycheva, O., Fransson, T., 2004. Flutter of the low pressure turbine blades with cyclic symmetric modes: a preliminary design method. *Journal of Turbomachinery*, 126(2), pp. 306-309. doi:10.1115/1.1650380.
- [5] Megerle, B., McBean, I., Rice T. S., Ott, P., 2012. Numerical and Experimental investigation of the Aerodynamic Excitation of a Model Low-Pressure Steam Turbine Stage Operating under Low Volume Flow, *ASME Turbo Expo*, paper GT2012-68384
- [6] Sanvito, M., Pesatori, E., Bachschmid, N., Chatterton, S., 2012. Analysis of LP steam turbine blade vibrations: experimental results and numerical simulations, *IMECHE VIRM Conference Proceedings*.

## ACKNOWLEDGMENT

The permission of Franco Tosi Meccanica S.p.A. to publish these results is gratefully acknowledged.